Accepted Manuscript

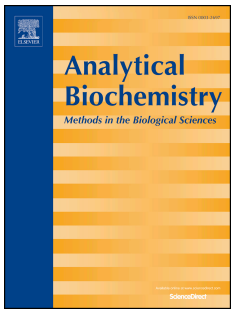

Amplified detection of streptomycin using aptamer-conjugated palladium nanoparticles decorated on chitosan-carbon nanotube

Rozita Aghajari, Azadeh Azadbakht

PII: S0003-2697(18)30103-9

DOI: 10.1016/j.ab.2018.02.005

Reference: YABIO 12929

To appear in: *Analytical Biochemistry*

Received Date: 28 November 2017

Revised Date: 5 February 2018

Accepted Date: 7 February 2018

Please cite this article as: R. Aghajari, A. Azadbakht, Amplified detection of streptomycin using aptamer-conjugated palladium nanoparticles decorated on chitosan-carbon nanotube, *Analytical Biochemistry* (2018), doi: 10.1016/j.ab.2018.02.005.

Amplified detection of streptomycin using aptamer-conjugated palladium nanoparticles decorated on chitosan-carbon nanotube

Rozita Aghajari, Azadeh Azadbakht[a]

[a]*Departmentof Chemistry, Khorramabad Branch, Islamic Azad University , Khorramabad, Iran.*

Abstract

A streptomycin-specific aptamer was used as a receptor molecule for ultrasensitive quantitation of streptomycin. The glassy carbon (GC) electrode was modified with palladium nanoparticles decorated on chitosan-carbon nanotube (PdNPs/CNT/Chi) and aminated aptamer against streptomycin. Modification of the sensing interface was characterized by scanning electron microscopy (SEM), energy-dispersive X-ray (EDS), wavelength-dispersive X-ray spectroscopy (WDX), cyclic voltammetry (CVs), and electrochemical impedance spectroscopy (EIS). The methodologies applied for designing the proposed biosensor are based on target-induced conformational changes of streptomycin-specific aptamer, leading to detectable signal change. Sensing experiments were performed in the streptomycin concentration range from 0.1 to 1500 nM in order to evaluate the sensor response as a function of streptomycin concentration. Based on the results, the charge transfer resistance (R_{ct}) values increased proportionally to enhanced streptomycin content. The limit of detection was found to be as low as 18 pM. The superior selectivity and affinity of aptamer/ PdNPs/CNT/Chi modified electrode for streptomycin recognition made it favorable for versatile applications such as streptomycin analysis in real samples.

Keywords: Aptasensor, Streptomycin, Palladium nanoparticles, Carbon nanotube.

*Corresponding author: A. Azadbakht, Tel: +98 6633120399
E-mail:Azadbakht.a@gmail.com

1. Introduction

Streptomycin is an aminoglycoside antibiotic mainly active against gram-negative bacteria; as a consequence, it has been extensively employed as an antibacterial drug in human therapy. Furthermore, owning to particular inhibition activity against above bacteria, it has been also utilized as a veterinary drug (especially in bee-keeping) in animal husbandry, and crop-preservation agents in agriculture [1, 2]. The bacterial protein synthesis is impaired in the presence of streptomycin due to its binding to prokaryotic ribosomes. Serious side effects for streptomycin over dosage have been recognized including allergic reactions, nephrotoxicity, loss of hearing and toxicity to the kidneys, etc. [3–5].

To date, several methods and strategies to assay and quantitative measurement of streptomycin have been applied. Immunochemical assays have been considered as an attractive method for the quantification of trace amount of targets with high specificity and sensitivity. Variety number of immunochemical assays, such as enzyme linked immuno-sorbent assay (ELISA), fluorescence immunoassay (FIA), and radioimmunoassay (RIA) have been reported for as screening tests for target molecules analysis [6-8]. However, their applications for assay of antibiotics residues have been restricted due to the cross-reactions with other substances in biological sample [9]. Furthermore, generation of antibodies for construction of immunochemical assays is time- consuming and costly. Therefore, along with these methods, more selective methods such as chromatography have been conventionally described for confirmatory analysis. Liquid chromatography-mass spectrometry (LC–MS) as a conventional method has been used for detection of streptomycin with high sensitivity, but the large amounts of volatile organic solvents used in the mobile phase make this technique as an undesirable method to most analysts. Besides, it is labor-intensive and expensive procedure [10, 11]. Moreover, high performance liquid chromatography (HPLC) has been introduced as high sensitive system for streptomycin detection but needs post-column derivatization owing to lack of chromophore group in streptomycin [12, 13]. Thus, developing the fast, accurate, reliable and efficient appraisal system for quantification assay of streptomycin is desirable for routine analysis.

To figure out many of these challenges, we have turned to the use of aptamers as specific recognition element. The sequence of aptamers can be chosen from libraries with up to 10^{15} different nucleotides by a procedure known as systematic evolution of ligands by exponential enrichment (SELEX) [14, 15]. Despite consisting of only 4 building blocks (nucleotides), the individual aptamers are able to recognize and bind targets with high affinity

specificity comparable to antibodies because of their ability to adopt unique three-dimensional structures [16]. Aptamers bear functional features in many cases similar to antibodies. In comparison with molecular probes for biomarker recognition and traditional antibodies, aptamers possess the intrinsic advantages including low cost, high specificity, low molecular weight, excellent thermal stability, easy and reproducible, versatility in application, easy manipulation, and lack of immunogenicity and toxicity [17-19]. Therefore, they are being used broadly in the miscellaneous field including diagnostics, therapeutics, research, separation and bioanalysis fields [20, 21].

Based on different transduction techniques, various aptasensors have been reported such as optical [22], luminescence [23], surface plasmon resonance [24], electrochemical [25] and piezoelectric [26] aptasensors. Relying on the promising properties of electrochemical detection schemes such as high sensitivity, low cost, inherent simplicity, and miniaturization, electrochemical aptamer-based sensors have attracted tremendous attention for biosensing [27]. In addition, signal amplification based on biofunctional nanomaterials for the fabrication of electrochemical aptasensor is extremely taken into consideration. Among different nanomaterials, carbon nanotube (CNT) has been widely used thanks to their excellent properties, such as high accessible surface area and electronic conductivity, good antifouling, reinforcing properties, biocompatibility and high stability. Also, noble metal nanoparticles including palladium nanoparticles (PdNPs) show novel electrocatalytic property, stability and biocompatibility for determination of biomolecule [28]. Chitosan (Chi) with amino (NH_2) and hydroxyl (OH) groups has a great opportunity to bind with biomolecules easily and can be cross-linked with crosslinking agents such as glutaraldehyde to prevent dissolution in acidic solutions [29]. Combinations of electrochemical aptasensor with different nanomaterials, such as CNT, PdNPs and Chi have been recently used for improving the performance of electrochemical sensors [30, 31].

In this report, we integrated the individual properties of PdNPs, Chi, CNT, and aminated aptamer against streptomycin for construction of high sensitive impedimetric aptamer assay for streptomycin detection. To this end, palladium nanoparticles decorated on chitosan-carbon nanotube (PdNPs/Chi/CNT) and streptomycin-aptamer were immobilized onto glassy carbon (GC) electrode via drop casting and covalent attachments. It was hypothesized that binding of the aptamer with target molecule results in a change of aptamer structure from an unstructured single stranded DNA to a three-way stem. The aptamer was used for streptomycin assay through electrochemical sensors and the faradaic impedance spectroscopy (FIS) was selected as transducer.

2.1 Chemicals

Multi-walled carbon nanotubes with 95% purity, diameters in the range of 10-15 nm, and 1 mm length were obtained from Nanolab (Brighton, MA). Acetic acid (CH_3COOH), nitric acid (HNO_3, 60%), sulfuric acid (H_2SO_4, 97%), potassium chloride (KCl), chitosan, potassium ferricyanide ($K_3Fe(CN)_6$), and potassium ferrocyanide ($K_4Fe(CN)_6$), were all bought from Merck (Germany) and Fluka. Palladium(II) chloride ($PdCl_2$), disodium phosphate (Na_2HPO_4), monosodium phosphate (NaH_2PO_4),streptomycin, and1-Ethyl- 3-(3-dimethylaminopropyl) carbodiimide hydrochloride (EDC) were prepared from Sigma-Aldrich. All aqueous solutions were prepared with double-distilled water. A specific 5'-amine-terminated aptamer against streptomycin with the sequence of 5'-NH_2-$(CH_2)_6$ TAG GGA ATT CGT CGA CGG ATC CGG GGT CTG GTG TTC TGC TTT GTT CTG TCG GGT CGT CTG CAG GTC GAC GCA TGC GCC G-3′ was adopted according to the reported study and used for determination of streptomycin in our experiments [32]. The DNA strand was synthesized and purified via high-performance liquid by Bioneer (South Korea) and were stored in nuclease-free water at −20 °C until use. All experiments were performed at ambient temperature of 25 ±1 ◦C.

2.2 Instruments and apparatus

All Electrochemical experiments were carried out on a computer controlled Autolab potentiostat/galvanostat (PGSTAT204, Eco-Chemie, the Netherlands). The experimental conditions were controlled with NOVA 1.8 and Frequency Response Analyzer (FRA) software. A conventional three-electrode electrochemical cell with a modified glassy carbon (GC) electrode as working electrode, a platinum foil as auxiliary electrode, and a saturated Ag/AgCl electrode as reference electrode were employed throughout the experiments. The morphology of nanocomposite, size and distribution of nanoparticles were investigated using the scanning electron microscopy microscope (SEM, X-30 Philips instrument). Moreover, the energy-dispersive X-ray spectroscopy (EDS) and wavelength-dispersive X-ray (WDX) spectroscopy were utilized by a Vega-Tescan electron microscope. Differential pulse voltammetry (DPV) signals were recorded in 0.1M PBS containing 5.0 mM $K_3[Fe(CN)_6]/K_4[Fe(CN)_6]$ (1:1) within the potential range from -0.3 to 0.7 V under a modulation amplitude of 0.05V, a pulse width of 0.05 s, sample width of 0.0167s and step potential of 0.001 mV. The electrochemical behavior of modified electrode was also assessed by recording the electrochemical impedance spectroscopy (EIS) response in 0.1M PBS and 5.0 mM $K_3[Fe(CN)_6]/K_4[Fe(CN)_6]$ (1:1) solution in the frequency range from 0.1 Hz and 100

kHz with 5 mV as signal amplitude and 0.2 V bias potential. All cyclic voltammetries (CVs) measurement were performed in the presence of $K_3[Fe(CN)_6]/K_4[Fe(CN)_6]$ (1:1) 5.0 mM and 0.1 M PBS by sweeping the potential between -0.8 V and + 0.8 V at 50 mV s^{-1}.

2.3 Electrode modification

Before each electrochemical experiment, GC electrode was polished with 0.3, and 0.05 mm alumina slurry in sequence, rinsed thoroughly with doubly distilled water between each polishing step, sonicated in 1:1 HNO_3/ethanol and doubly distilled water, and dried at room temperature. The construction processes of the modified electrode are described as following proceedings. The proper amount of chitosan flakes was dissolved in acetic acid solution (2% (v/v), 2 mL). 5.0 mg CNT were dispersed in 2.0 ml of 2% chitosan medium and solution gently sonicated until homogenous suspension was obtained. GC electrode was modified by a drop of 6 μL CNT/chitosan dispersion. The modified electrode allowed to dry for 15 min (the resulting electrode is called CNT/Chi/GC electrode). PdNPs/CNT/Chi platform were easily fabricated by a potentiostatic method [33]. To this end, the CNT/Chi/GC electrode was immersed in 0.5 M H_2SO_4solution containing 0.01 M $PdCl_2$. Pd^{+2} adsorbed on the CNT/Chi film were changed into PdNPs without any additives in a simple one-step procedure using an applied potential of -0.3 V within 300 s at room temperature for 400 s at –0.2 V.

2.4 Preparation of aptamer/CNT/Chi/PdNPs modified electrode

Once the PdNPs/CNT/Chi layer was dried, it was allowed to react with glutaraldehyde solution for 2 s. After the electrodeposition processes, the modified sensing layer were gently washed in water and air-dried at room temperature. The last step of sensing interface fabrication was aptamer adherence. The strand DNA sequence was immobilized at the surface of modified electrode by incubating the electrode with mixed solution of 1 mM EDC and 10 μL amine functionalized streptomycin-aptamer prepared in phosphate buffer solution. The oligonucleotide was covalently attached to the aldehyde groups coming from the glutaraldehyde layer immobilized at the electrode surface. Finally, the developed aptasensor (hereafter denoted as aptamer/PdNPs/CNT/Chi) was thoroughly rinsed with ultrapure water in order to remove unbound aptamers. Every step in the construction of aptasensor was verified by electrochemical characterization using CV and EIS. To make a comparison between applicability and functionality of different sensing layer, Chi/GC, CNT/Chi/GC were also prepared. For this purpose, electrodeposition process of chitosan was

performed by immersing the GC and CNT/GC electrodes into a 0.2% (W/V) chitosan solution and applying the potential pulses of -2.5 V for 300 s [34].

2.5 EIS Measurements of Surfaces

In order to evaluate aptamer- streptomycin interactions, the designed aptasensor was treated with various content of streptomycin as a target molecule for 30 min. In the subsequent step, the R_{ct} value of modified electrode was recorded in the solution containing 5.0 mM $[Fe(CN)_6]^{3-/4-}$ and 0.1M PBS, as mentioned in the preceding section. The surface modification scheme and streptomycin mechanism quantification are shown in Fig. 1. As shown in Fig. 1, incubation the sensing interface with streptomycin caused a dramatic increase of R_{ct} value to about 780 Ω, whereas when the aptasensor was incubated with solution without streptomycin, the minimal charge transfer resistance was achieved (102 Ω). This phenomenon can be ascribed to streptomycin capture on aptamer-functionalized surfaces. In fact, streptomycin was caught by affinity binding to the surface-linked aptasensor and the analyte-induced increment of the impedance was employed to determine streptomycin. Owning to steric hindrance caused by formation of streptomycin-aptamer at the sensing platform, the electron transfer of $[Fe(CN)_6]^{3-/4-}$ probe precluded, resulting in the measurable increased R_{ct} value.

3. Results and discussion

3.1 Characterization of sensing interface

Scanning electron microscope (SEM) is used to reveal the size, morphology and structure of prepared products. Also the elemental analysis was performed by energy-dispersive X-ray spectroscopy (EDS). SEM micrographs analyze of bare GC (A), CNT/GC (B), CNT/Chi/GC (C), and PdNPs/CNT/Chi/GC (D) electrodes are shown in Fig. 2. It can be clearly observed that the CNT/Chi composite has a flake structure, while the spaghetti-like CNT are spread out in the chitosan matrix (magnification in Fig. 2C). As illustrated in Fig.2C, great amount of Chi grafted onto the whole CNT surface. When the CNT/Chi was decorated with PdNPs, the composite covered with the spherical PdNPs (Fig. 2D), verifying that the PdNPs/CNT/Chi had been successfully synthesized. The quantitative analyses of these spectra were carried out by using EDS analysis. The presence of Pd, C, O, and N elements in the PdNPs/CNT/Chi/GC are proved by using EDS signal. As can be obviously seen from Fig. S1A, the EDS spectra PdNPs/CNT/Chi nanocomposite exhibit peaks characteristic of the Pd element, evidencing that the Pd element existence in the electrode surface. The WDX images give further evidences for presence of the Pd, C, O, and N in the

nanocomposite. WDX images represented the distribution of Pd, C, O, and N (Fig. S1B-S1E, respectively).

3.2 Optimum concentration of streptomycin-aptamer

In the first set of experiments, the relationship between aptamer concentration and the changes of R_{ct} value intensity (ΔR_{ct}) was explored. The sensing interfaces were prepared by immobilization aptamer concentrations ranging from 0.5 to 10 μM at the surface of PdNFs/CNT/Chi/GC electrode. The R_{ct} values of each device without incubation in the streptomycin solution were also served as control experiments. All modified aptasensors were then challenged with the same concentration of streptomycin and the electrochemical response of all aptasensors recorded in the solution containing 5.0 mM $[Fe(CN)_6]^{3-/4-}$ and 0.1M PBS after treating with the streptomycin were obtained. Based on the Fig.3, the ΔR_{ct} were observed to increase with aptamer concentration up to 5 μM and then decrease as the rise of aptamer concentration. This phenomenon could be related to the inactivation of some aptamers due to undesirable interactions between aptamers in the vicinity of each other such as cross hybridization [35]. Taking all above explanation into account, 5 μM was chosen as optimized aptamer concentration throughout experiments.

3.3 Optimum pH value

To examine the influence of the pH on the properties of designed aptasensor, the incubation solution containing equal amount of streptomycin in different pH values were served. The electrochemical signal of aptasensor before and after incubation in the solution containing constant amount of streptomycin in different pH values were monitored. Based on the Fig. 4, the ΔR_{ct} obviously increase by increasing pH value from 4 to 7. With further increase of the pH value, the variation of electrochemical signal was attenuated. So the pH value of 7 was chosen for prepration of incubation solution in subsequent experiments. This phenomenon can be ascribed to this fact that in the strong acidic and alkaline solutions disadjust the aptamer-target complex formation, decrease the affinity between aptamer and the target molecules, and also influence the folding of aptamer.

3.4 Optimum incubation time of streptomycin

Reaction time between streptomycin and aptamer on the PdNPs/CNT/Chi/GC interface was also optimized for different lengths of time using DPV technique (Fig. 5). ΔI recorded for aptamer/PdNPs/CNT/Chi/GC electrode before and after incubation the aptasensor in the solution containing 50 nM streptomycin for various incubation times. By

taking the ΔI value into consideration, it can be clearly concluded that the change of current response value increased with increasing the interaction time from 5 min to 30 min and then reaches a plateau in 40 min. This behavior can be interpreted in terms of the formation of a tertiary structure of aptamer-target cells at 30 min. Thus, 30 min of incubation was chosen for the further experiments.

3.5 Electrochemical behavior of aptasensor

In order to trace the construction operations of the aptasensor, the CV and EIS were served as effectual methods to probe the interfacial properties of a modified electrode in different steps. Fig. 6A depicts the CVs of 5.0 mM $[Fe(CN)_6]^{3-/4-}$ redox couple in 0.1M PBS at scan rate of 50 mV s^{-1} on the bare GC, Chi/GC, CNT/Chi/GC, PdNP/CNT/Chi/GC, and aptamer/PdNP/CNT/Chi/GC electrodes. As can be seen in Fig 6A and 6B, the anodic peak current of the bare GC electrode was 521 μA and the ΔE_p was estimated to be about 210 mV. By electrodeposition the GC electrode with chitosan the peak current of $[Fe(CN)_6]^{3-/4-}$ redox probe notably decreased with increase in ΔE_p, which demonstrates that the electron transfer kinetics were restricted. After immobilization the CNT/Chi at the surface of bare GC electrode, the CV curve indicated a considerable increase in the peak current of $[Fe(CN)_6]^{3-/4-}$ compared with Chi/GC electrode, which can be associated with the improvement of electron transfer. Also the electrochemical redox reversibility of $[Fe(CN)_6]^{3-/4-}$ redox couple at CNTs/Chi/GC electrode was better than that at Chi/GC surface. The value of anodic current signal of $[Fe(CN)_6]^{3-/4-}$ revealed the significant increase after electrodeposition of PdNPs at the surface of CNT/Chi/GC electrode, verifying the promotion of electron transfer capability between sensing platform and $[Fe(CN)_6]^{3-/4-}$ probe. The PdNPs/CNT/Chi nanocomposite not only has been served for current signal promotion but also employed for aptamers immobilization. The utilizing of chitosan in the nanocomposite structure was mainly for the attachment of the streptomycin aptamers on the sensing interface through the covalent bonding interaction between the amino groups on the chitosan and the aldehyde groups in glutaraldehyde. The aptamer immobilization was performed by interaction the aldehyde groups at the other end of glutaraldehyde with the NH_2 terminus of aptamer. Although aptamer has been introduced to be absorbed on the surface of CNT via π- π interaction, herein, the amino groups on nanocomposite could help the aptamer loaded on the surface of the modified electrode mainly via the strong covalent bonds rather than the π- π interaction [36]. Obviously, the strong amide bonds have been known to be superior to π- π weak interaction. The real reason to use covalent bonds here over π- π interaction should be better interaction between aptamer and streptomycin. When π- π interaction is used for anchoring,

single stranded DNA will be lying flat on CNT surface which will limit its recognition with target molecule. The CVs response of PdNPs/CNT/Chi/GC electrode after aptamer attachments was also recorded. As can be seen clearly, the peak current of $[Fe(CN)_6]^{3-/4-}$ redox couple decreased obviously, indicating that the diffusion of $[Fe(CN)_6]^{3-/4-}$ to the electrode surface has been prevented.

Also, the electrochemical properties of a bare GC electrode and those after each step of modification, including coating with Chi, CNT/Chi, PdNPs/CNT/Chi, and aptamer/PdNPs/CNT/Chi were studied using EIS method. Faradaic impedance spectra were recorded as a Nyquist plot and data were adjusted to a Randles equivalent circuit. According to Fig.S2 the R_{ct} value for different step of modification processes was found to be in the order of Chi/GC > aptamer/PdNP/CNT/Chi/GC > CNT/Chi/GC > bare GC> PdNPs/CNT/Chi/GC. The EIS measurement results were consistent with those obtained from the CV measurements and clearly confirmed fabrication of the aptasensor.

3.6 Analytical performance

To evaluate the applicability of aptamer/PdNPs/CNT/Chi electrode for the accurate quantification of target molecule, the EIS Nyquist signal of modified electrode was recorded at various concentrations of streptomycin under optimal experimental conditions. The results indicate that as the concentration of the target molecule increases, the R_{ct} value progressively increases (Fig. 7A). The increasing of charge transfer resistance is ascribable to the particular interaction between aptamer and streptomycin. The semicircle diameter of the Nyquist plot reaches a plateau by increasing the concentration of the streptomycin to 2500 nM. This is attributed to the occupation of all the aptamer sites on the sensing layer by the target molecule. The calibration curve was constructed by plotting the aptasensor response versus the concentrations of the streptomycin as shown in Fig. 7B. The calibration curve showed linear relationship over the range from 0.1 – 1500 nM, showing a correlation coefficient of 0.995. The limit of detection (LOD) was calculated to be as low as 18 pM based on $3\sigma/b$, where σ is the standard deviation of the blank samples and b is the slope of the calibration curve. The comparison results of the analytical performance of our constructed aptasensor with some other detection methods are given in Table. 1. Based on tabulated results, the analytical parameters for aptamer/PdNPs/CNT/Chi aptasensor are comparable to or better than the results reported for streptomycin determination at the surface of other modified electrodes [37 - 43].

3.7 Real sample analysis

To verify the compatibility of our device with biological fluids, the constructed sensor was used to measure streptomycin in milk containing a mixture of many different proteins and other interfering materials. Milk is considered as one of the most important regulated products in food analysis due to the risk of having veterinary medicine residue. Therefore, introducing the method for streptomycin assay in milk has received considerable attention. The commercial milk sample with 5.0% fat was procured from local market. Combination of several sample pre-treatment techniques such as centrifugation, filtration, and dilution of milk with PBS was carried out for real sample analysis. In brief, the milk samples were centrifuged at 6000 rpm for 25 min at room temperature and filtered with 0.22 mm filter and diluted with PBS with the proportional of 1:50. In the sequence steps, streptomycin standard solutions were spiked into the diluted milk to have the streptomycin content of 2.5, 5.0, 8.0 and 10.0 nM. Based on the results, the recovery in the range of 93.6 – 102.2 % was calculated.

3.8 Specificity of the electrochemical aptasensor

To better characterize specificity of the electrochemical aptasensor, the functionalized surfaces were challenged with some common interferences. Experiments aimed at challenging surfaces with various interfering species with 1000-fold higher concentration than the streptomycin content. Surfaces containing DNA streptomycin aptamer were first shown to be specific for binding streptomycin antibiotic and were subsequently used for capture of analogous compounds as interferences. The high selectivity of the aptamer was apparent from Fig. 8. As shown in Fig. 8, the variation of charge transfer resistance value were negligible by the addition of interferences including glucose, ascorbic acid, tetracycline, penicillin, and amoxicillin, compared with ΔR_{ct} caused by streptomycin addition. So, a dramatic variation of binding affinity is observed because none of the analogous compounds examined were able to induced conformational changes of streptomycin-specific aptamer even at μM concentrations.

3.9 Stability and reproducibility of the aptasensor

The stability of the electrochemical aptasensor is a crucial factor in practical applications. The stability of our electrochemical aptasensor was investigated in a solution of 5.0 mM $[Fe(CN)_6]^{3-/4-}$ and 0.1M PBS, by recording consecutive CVs from -0.8 V and + 0.8 V vs. Ag/AgCl reference electrode at 50 mV s^{-1}. As demonstrated in Fig. 9, the unchanged redox peaks of $[Fe(CN)_6]^{3-/4-}$ after 25 cycles suggest that aptamer/PdNPs/CNT/Chi sensor is strongly stable. The long term stability of proposed aptasensor was evaluated by storing the

sensor at 4 °C. According to the results, after 3 weeks just 6.4 % decrease in its initial activity was observed, stating good stability of the aptamer/PdNPs/CNTs/Chi sensor.

The reproducibility of this analytical approach for the detection of 10 nM streptomycin was investigated by recording the EIS response of four electrodes in a solution of 0.1M PBS containing 5.0 mM $[Fe(CN)_6]^{3-/4-}$. The summarized results were given in Table S1. According to results, acceptable relative standard deviations (RSD) of the prepared aptasensors responses were obtained 3.7%, which indicated that high reproducibility of sensor.

4 Conclusion

The goal of the present paper was to fabricate and characterize functionalized surfaces for capture of streptomycin. Our experiments show that surfaces functionalized with aptamers can be considered as effective interface in capturing streptomycin. This strategy was introduced based on using PdNPs/CNT/Chi nanocomposite as a signal amplifier and target-induced conformational change in the streptomycin aptamer structure. The PdNPs/CNT/Chi interface not only has been used for current signal amplification but also served for streptomycin-aptamers immobilization via the covalent bonding between amino groups on the chitosan and aldehyde groups of linker. Owning to the larger surface area of employed nanocomposite and abundant $–NH_2$ groups in nanocomposite, a large numbers of streptomycin-aptamers were captured on sensor interface, thus amplifying the detection signal was observed. Under the optimum condition, the charge transfer resistance of aptasensor linearly increased by the addition of streptomycin in concentration ranges of 0.1-1500 nM and the estimated detection limit was found to be 18 pM. The described protocol has several attractive advantages including simplicity, fast response, efficient sensitivity, high selectivity, and no requirement for a specific label.

Acknowledgements

The authors gratefully acknowledge the support of this work by the Khorramabad Branch, Islamic Azad University for financial support.

[1] M. van Bruijnsvoort, S. J. M. Ottink, K. M. Jonker, E. de Boer, Determination of streptomycin and dihydrostreptomycin in milk and honey by liquid chromatography with tandem mass spectrometry, J. Chromatogr. A 1058 (2004) 137–142. doi: org/10.1016/j.chroma.2004.07.101

[2] J. P. Ferguson, G. A. Baxter, J. D. G. McEvoy, S. Stead, E. Rawlings, M. Sharman, Detection of streptomycin and dihydrostreptomycin residues in milk, honey and meat samples using an optical biosensor, Analyst 127 (2002) 951–956. doi:10.1039/B200757F

[3] T. M. Wassenaar, Use of Antimicrobial Agents in Veterinary Medicine and Implications for Human Health, Crit. Rev. Microbiol. 31 (2005) 155–169. doi: org/10.1080/10408410591005110

[4] H. C. Wegener, Antibiotics in animal feed and their role in resistance development, Curr. Opin. Microbiol. 6 (2003) 439-445. doi: org/10.1016/j.mib.2003.09.009

[5] R. Krieger, Handbook of Pesticide Toxicology, Principles, Part 1, Academic Press, San Diego, CA, 2001.

[6] N. Pastor-Navarro, A. Maquieira, R. Puchades, Review on immunoanalytical determination of tetracycline and sulfonamide residues in edible products, Anal. Bioanal. Chem. 395(2009) 907-920. doi: 10.1007/s00216-009-2901-y

[7] S. Reberaz, M. G. E. G. Bremer, W. Haasnoot, W. Norde, Label-free and multiplex detection of antibiotic residues in milk using imaging surface plasmon resonance-based immunosensor, Anal. Chem. 81(2009) 7743-7749. doi: 10.1021/ac901230v

[8] N. A. Byzova, E. A. Zvereva, A. V. Zherdev, S. A. Eremin, P. G. Sveshnikov, B. B. Dzantiev, Pretreatment-free immunochromatographic assay for the detection of streptomycin and its application to the control of milk and dairy products, Anal. Chim. Acta 701(2011) 209-217. doi: org/10.1016/j.aca.2011.06.001

[9] S. Jongberg, V. Orlien, L. H. Skibsted, S. Weigel, Elimination of matrix interferences in biosensor analysis of streptomycin in honey, Eur. Food Res. Technol. 228 (2009) 659–664. doi: 10.1007/s00217-008-0975-y

[10] A. M. Gremilogianni, N. C. Megoulas, M. A. Koupparis, Hydrophilic interaction vs ion pair liquid chromatography for the determination of streptomycin and dihydrostreptomycin residues in milk based on mass spectrometric detection, J. Chromatogr. A, 1217 (2010) 6646–6651. doi: org/10.1016/j.chroma.2010.04.059

[11] L.G. McLaughlin, J.D. Henion, P.J. Kijak, Multi-residue confirmation of aminoglycoside antibiotics and bovine kidney by ion spray high-performance liquid chromatography/tandem mass spectrometry, Biol. Mass. Spectrom. 23(1994) 417–429. doi: 10.1002/bms.1200230706

[12] P. Edder, A. Cominoli, C. Corvi, Determination of streptomycin residues in food by solid-phase extraction and liquid chromatography with post-column derivatization and fluorometric detection, J. Chromatogr. A. 830 (1999) 345–351. doi: org/10.1016/S0021-9673(98)00917-0

[13] N. Zhou, J. Wang, J. Zhang, C. Li, Y. Tian, J. Wang, Selection and identification of streptomycin-specific single-stranded DNA aptamers and the application in the detection of streptomycin in honey, Talanta 108 (2013)109–116. doi: org/10.1016/j.talanta.2013.01.064

[14] R. Stoltenburg, C. Reinemann, B. Strehlitz, SELEX-A (r) evolutionary method to generate high-affinity nucleic acid ligands, Biomol. Eng. 24 (2007) 381-403. doi: org/10.1016/j.bioeng.2007.06.001

[15] C. Tuerk, L. Gold, Systematic evolution of ligands by exponential enrichment: RNA ligands to bacteriophage T4 DNA polymerase, Science, 249(1990) 505-510.

[16] A. D. Ellington, J. W. Szostak, In vitro selection of RNA molecules that bind specific ligands, Nature 346 (1990) 818- 822. doi:10.1038/346818a0

[17] D. P. Xie, C. C. Li, S. G. Li, H. L. Qi, D. Dong, Q. Gao, C. X. Zhang, Click chemistry-assisted self-assembly of DNA aptamer on goldnanoparticles-modified screen-printed carbon

electrodes for label-free electrochemical aptasensor, Sens. Actuat. B 192 (2014) 558–564. doi: org/10.1016/j.snb.2013.11.038

[18] Y. Lian, F. He, H. Wang, F. Tong, A new aptamer/graphene interdigitated goldelectrode piezoelectric sensor for rapid and specific detection of Staphylococcus aureus, Biosens. Bioelectron. 65(2015) 314–319. doi: org/10.1016/j.bios.2014.10.017

[19] F. Ma, C. Ho, K.H.C. Alan, H.Z. Yu, Immobilization of redox-labeled hairpin DNA aptamers on gold: electrochemical quantitation of epithelial tumor marker mucin 1, Electrchim. Acta, 110 (2013)139-145. doi: org/10.1016/j.electacta.2013.02.088

[20] D. H. Bunka, P. G. Stockley, Aptamers come of age- at last, Nat. Rev. Microbiol. 4 (2006) 588-596. doi:10.1038/nrmicro1458

[21] A. B. Iliuk, L. Hu, W. A. Tao, Aptamer in bioanalytical applications, Anal. Chem. 83 (2011) 4440- 4452. doi: 10.1021/ac201057w.

[22] M. Lee, D.R. Walt, A fiber-optic microarray biosensor using aptamers as receptors, Anal. Biochem. 282 (2000) 142–146. doi:org/10.1006/abio.2000.4595

[23] J. Wang, Y. X. Jiang, C. S. Zhou, X. H. Fang, Aptamer-based assay using aluminescent light switching complex, Anal. Chem. 77(2005) 3542–3546. doi: 10.1021/ac050165w

[24] A. Vasilescu, S. Gaspar, I. Mihai, A. Tache, S.C. Litescu, Development of a label-free aptasensor for monitoring the self-association of lysozyme, Analyst 138(2013) 3530–3537. doi: 10.1039/C3AN00229B

[25] A. Radi, J. L. Acero Sánchez, E. Baldrich, C.K. O'Sullivan, Reusable impedimetric aptasensor, Anal. Chem. 77 (2005) 6320–6323. doi: 10.1021/ac0505775

[26] B. R. Srijanto, C. P. Cheney, D. L. Hedden, A. C. Gehl, P. B. Crilly, M. A. Huestis, ,Piezoresistive microcantilevers-based cocaine biosensors, Sens. Lett. 10 (2012)850–855. doi: 10.1166/sl.2012.2335

[27] L. Li, F. Yang, X. R. Yang, Electrochemical luminescence detection based on ruthenium(II) tris (bipyridine) immobilized in sulfonic-functionalised titanianano-particles by ion exchange strategy. Analyst, 134(2009) 2100–2105. doi: 10.1039/B903434J

[28] G. Gao, D. Guo, H. Li, Electrocatalytic oxidation of formaldehyde on palladium nanoparticles supported on multi-walled carbon nanotubes, J. Power Sources, 162 (2006) 1094-1098. doi:org/10.1016/j.jpowsour.2006.07.057.

[29] A. Celik, A. Dincer, T. Aydemir, Characterization of β-glucosidase immobilized on chitosan-multiwalled carbon nanotubes (MWCNTS) and their application on tea extracts for aroma enhancement, Int. J. Biol. Macromol. 89 (2016) 406–414. doi:org/10.1016/j.ijbiomac.2016.05.008

[30] F. Shahdoost-fard, A. Salimi, E. Sharifi, A. Korani, Fabrication of a highly sensitive adenosine aptasensor based on covalent attachment of aptamer onto chitosan–carbon nanotubes–ionic liquid nanocomposite, Biosens. Bioelectron. 43 (2013) 100–107. doi:org/10.1016/j.bios.2013.03.060

[31] G. Hu, L. Chen, Y. Guo, S. Shao, X. Wang, Selective electrochemical sensing of calcium dobesilate based on the nano-Pd/CNTs modified pyrolytic graphite electrode, Talanta 78 (2009) 1211–1214. doi:org/10.1016/j.talanta.2008.12.071

[32] J. Yin, W. Guo, X. Qin, J. Zhao, M. Pei, F. Ding, A sensitive electrochemical aptasensor for highly specific detection of streptomycin based on the porous carbon nanorods and multifunctional graphene nanocomposites for signal amplification, Sens. Actuat. B 241 (2017) 151–159. doi: org/10.1016/j.snb.2016.10.062

[33] L. Abolghasemi Fard, R. Ojani, J. B. Raoof, Electrodeposition of three-dimensional Pdnanoflowers on a PPy@MWCNTs with superior electrocatalytic activity for methanol electrooxidation, Int. J. Hydrogen. Energ. 41 (2016) 17987-17994. doi: org/10.1016/j.ijhydene.2016.08.010

[34] S. Rajabzadeh, G. H. Rounaghi, M. H. Arbab-Zavar ,N. Ashraf, Development of a dimethyldisulfide electrochemical sensor based on electrodeposited reduced graphene oxide-chitosan modified glassy carbon electrode, Electrochim. Acta 135(2014) 543–549. doi: org/10.1016/j.electacta.2014.05.064

[35] S. Khezrian , A. Salimi, H. Teymourian, R. Hallaj, Label-free electrochemical IgE aptasensor based on covalent attachment of aptamer onto multiwalled carbon nanotubes/ionic liquid/chitosan nanocomposite modified electrode, Biosens. Bioelectron. 43(2013) 218–225. doi: org/10.1016/j.bios.2012.12.006

[36] X. Qin, Y. Yin, H.J. Yu, W.J. Guo, M.S. Pei, A novel signal amplification strategyof an electrochemical aptasensor for kanamycin, based on thioninefunctionalized graphene and hierarchical nanoporous PtCu, Biosens. Bioelectron. 77 (2016) 752–758. doi: org/10.1016/j.bios.2015.10.050

[37] J. Yina, W. Guo, X. Qin, J. Zhao, M. Pei, F. Ding, A sensitive electrochemical aptasensor for highly specific detection of streptomycin based on the porous carbon nanorods and multifunctional graphene nanocomposites for signal amplification, Sens. Actuat. B. 241(2017) 151–159. doi: org/10.1016/j.snb.2016.10.062

[38] X. Xu, D. Liu, L. Luo, L. Li, K. Wang, T. You, Photoelectrochemical aptasensor based on CdTe quantum dots-single walled carbon nanohorns for the sensitive detection of streptomycin, Sens. Actuat. B 251 (2017) 564–571. doi: org/10.1016/j.snb.2017.04.168

[39] G. K. Mishra, A. Sharma, S. Bhand, Ultrasensitive detection of streptomycin using flow injection analysis-electrochemical quartz crystal nanobalance (FIA-EQCN) biosensor, Biosens. Bioelectron. 67 (2015) 532-539. doi: org/10.1016/j.bios.2014.09.033

[40] B.Q. Liu, D.P. Tang, B. Zhang, X.H. Que, H.H. Yang, G.N. Chen, Au(III)-promoted magnetic molecularly imprinted polymer nanospheres for electrochemical determination of streptomycin residues in food, Biosens. Bioelectron. 41 (2013) 551–556. doi: org/10.1016/j.bios.2012.09.021

[41] N. Zhou, J. Wang, J. Zhang, C. Li, Y. Tian, J. Wang, Selection and identification of streptomycin-specific single-stranded DNA aptamers and the application in the detection of streptomycin in honey, Talanta 108 (2013) 109–116. doi: org/10.1016/j.talanta.2013.01.064

[42] A. Sarreshtehdar Emrani, N. M. Danesh, P. Lavaee, M. Ramezani, K. Abnous, S. M. Taghdisi, Colorimetric and fluorescence quenching aptasensors for detection of streptomycin in blood serum and milk based on double-stranded DNA and gold nanoparticles, Food Chemistry 190 (2016) 115–121. doi: org/10.1016/j.foodchem.2015.05.079

[43] B. Du, H. Li, J. Jin, T. Wang, Y. Li, G. Shen, X. Li, Chemiluminescence determination of streptomycin in pharmaceutical preparation and its application to pharmacokinetic study by a flow injection analysis assembly, 115 (2013) 823–828. doi: org/10.1016/j.saa.2013.07.007.

Fig.1 Schematic representation of different steps of aptasensor fabrication.

Fig. 2 Typical SEM micrographs analyze of bare GC (A), CNT/GC (B), CNT/Chi/GC(C), and PdNPs /CNT/Chi/GC (D).

Fig. 3 The variation of charge transfer resistance of aptasensor before and after incubation in the solution containing streptomycin (ΔR_{ct}) versus aptamer concentration.

Fig. 4 The variation of charge transfer resistance of aptasensor before and after incubation in the solution containing streptomycin (ΔR_{ct}) in different pH values.

Fig. 5 The variation of current value for aptamer/PdNPs/CNT/Chi/GC electrode before and after incubation in the solution containing streptomycin (ΔI) for various incubation times.

Fig. 6 (A) CVs for bare GC, Chi/GC, CNT/Chi/GC, PdNP/CNT/Chi/GC, and aptamer/PdNP/CNT/Chi/GC electrodes recorded in 0.1 M PBS containing 5.0 mM $[Fe(CN)_6]^{3-/4-}$. (B) The variation of current value for different electrodes.

Fig. 7 (A) Nyquist plots for aptamer/PdNPs/CNT/Chi/GC electrode recorded in solution containing 5.0 mM $[Fe(CN)_6]^{3-/4-}$ and 0.1M PBS after incubation with different concentration of streptomycin: 0, 0.1, 1, 10, 100, 200, 300, 450, 600, 800 and 1500 nM. (B) Plots of R_{ct} vs. streptomycin concentrations.

Fig. 8 EIS responses of prepared aptasensor before (curve a) and after (curve b) being incubated in the solution containing 200 μM glucose, ascorbic acid, tetracycline, penicillin, amoxicillin, and 200 nM streptomycin recorded in solution containing 5.0 mM $[Fe(CN)_6]^{3-/4-}$ and 0.1M PBS.

Fig. 9 Stability of the modified electrode tested by 25 repetitive potential sweeps at a scan rate of the 50 mV s^{-1} in the solution containing 5.0 mM $[Fe(CN)_6]^{3-/4-}$ and 0.1M PBS.

Table 1 Comparison between analytical performance of this method and other reported techniques for detection of streptomycin.

Electrode and sensor	Technique	LOD	Linear range	Refs.
GR[1]-Fe_3O_4-AuNPs/PCNR[2]/GCE[3]	DPV[4]	48.0 pM	85.0 pM - 343 nM	[37]
Aptamer/CdTe-SWCNHs[5]/ITO[6]	PEC[7]	33.0 pM	0.10 -50.0 nM	[38]
TGQC[8] surface	FIA-EQCN[9]	0.51 nM	0.51 – 85.0 nM	[39]
MIP[10]-based sensor	-	17.1 pM	85.0 pM - 34.3 nM	[40]
Aptamer/AuNPs surface	Colorimetric	-	0.20 – 12.0 μM	[41]
Aptamer/Cs dsDNA[11]	Fluorescence	47.6 nM (	Up to 2000 nM	[42]
NBS[12]/ eosin	CL[13]	3.80 nM	13.7 nM – 1.71 μM	[43]
This work	EIS[14]	18.0 pM	0.10 - 1500 nM	-

1: Graphen
2: Porous carbon nanorods
3: Glassy carbon electrod
4: Differential Pulse Voltammetry
5: Single walled carbon nanohorns
6: Indium tin oxide
7: Photoelectrochemical
8: Thiol modified gold quartz crystal
9: Flow injection analysis-electrochemical quartz crystal nanobalance
10: Molecularly imprinted polymer
11: Complementary strand
12:N-bromosuccinimide
13: Chemiluminescence
14: Electrochemical impedance spectroscopy

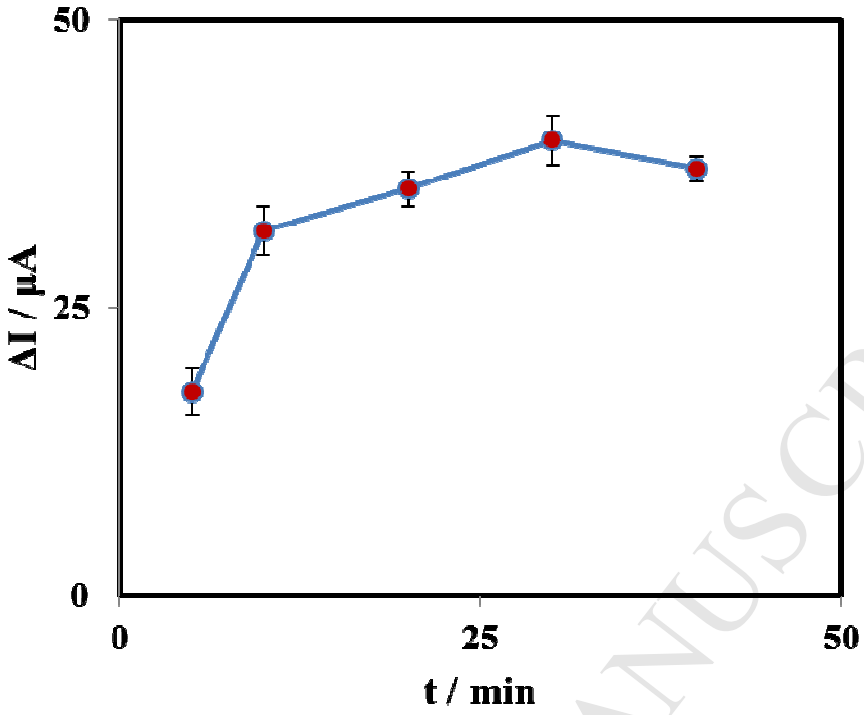

Fig. 5

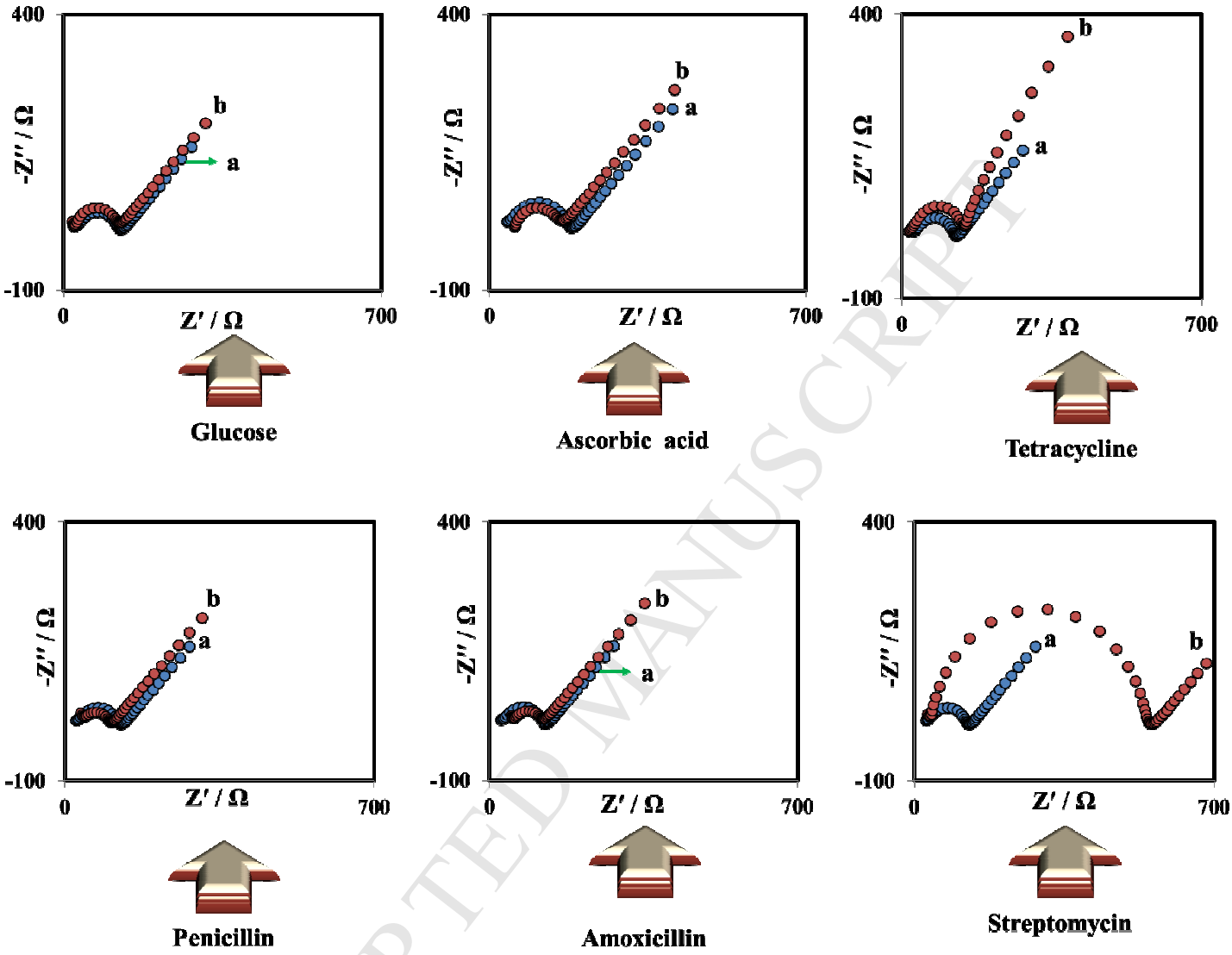

Fig. 8

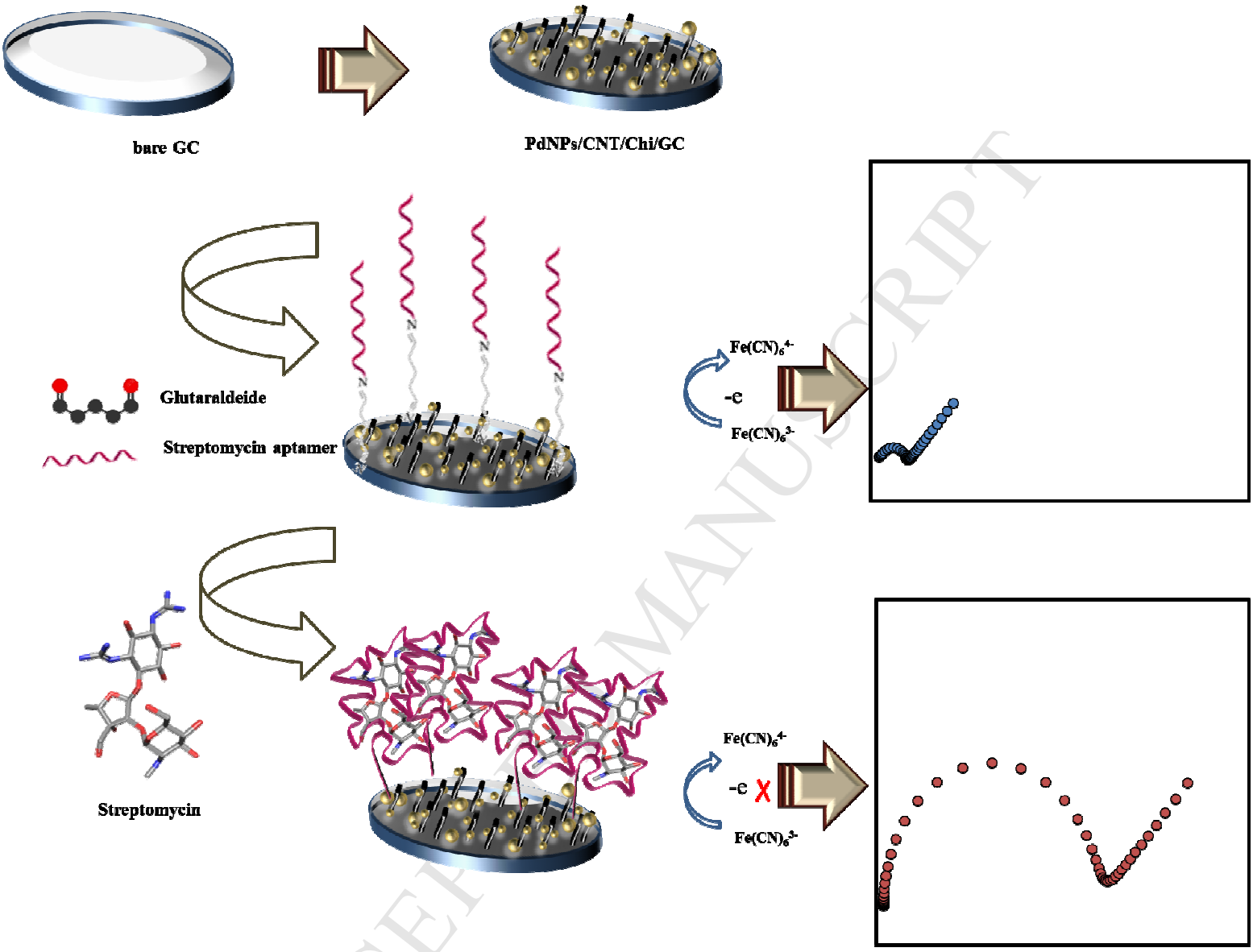

Fig. 1

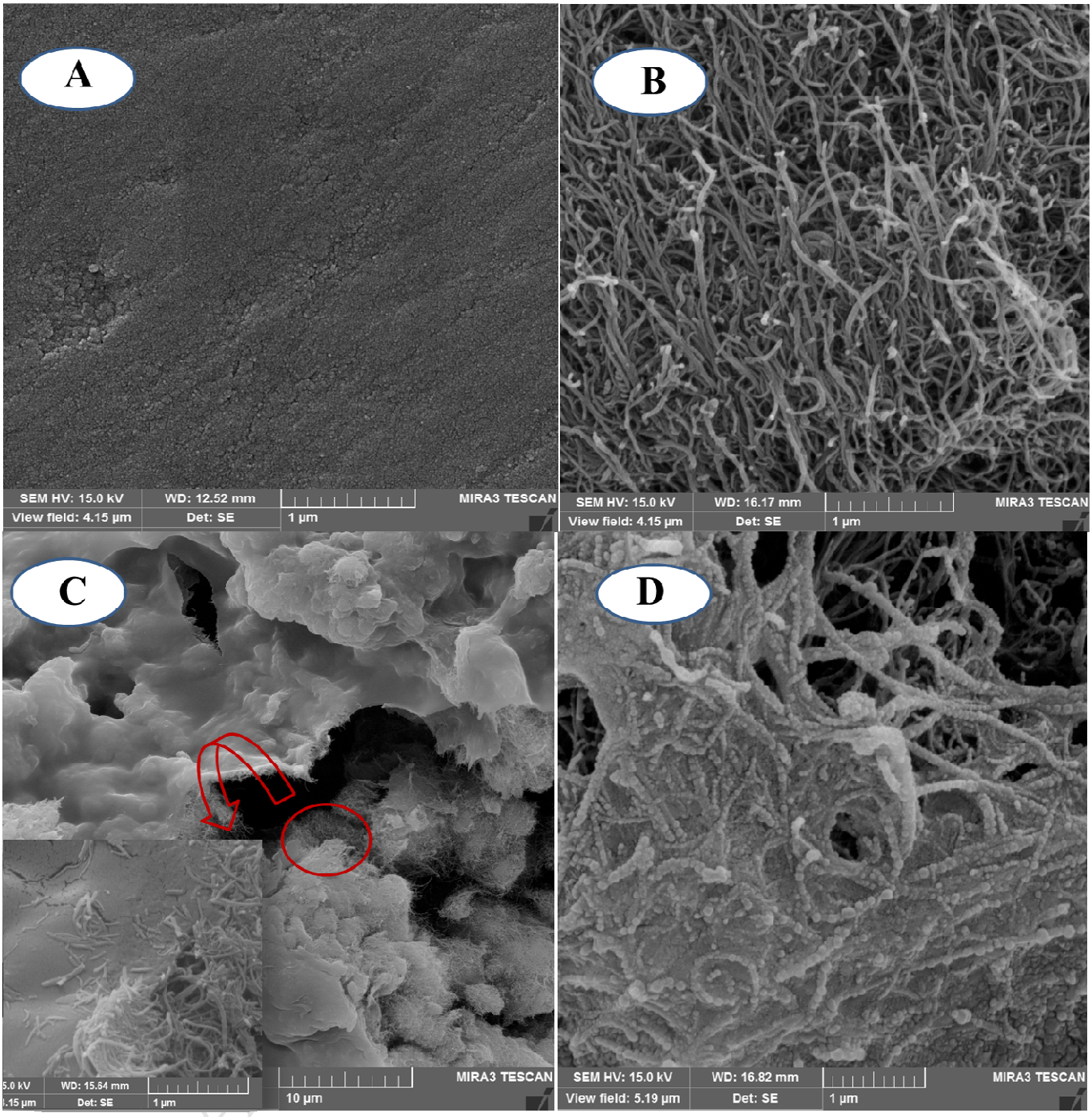
A
SEM HV: 15.0 kV
WD: 12.52 mm
View field: 4.15 µm
Det: SE
1 µm
MIRA3 TESCAN
B
SEM HV: 15.0 kV
WD: 16.17 mm
View field: 4.15 µm
Det: SE
1 µm
MIRA3 TESCAN
C
10 µm
MIRA3 TESCAN
D
SEM HV: 15.0 kV
WD: 16.82 mm
View field: 5.19 µm
Det: SE
1 µm
MIRA3 TESCAN

Fig. 2

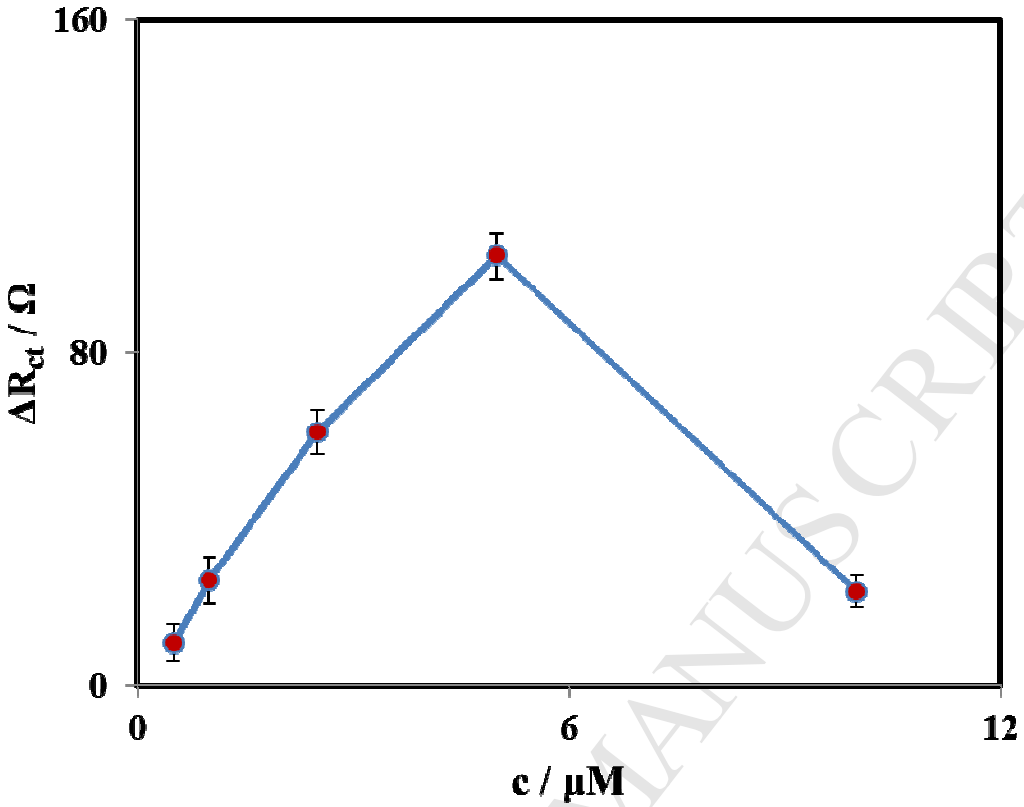

Fig. 3

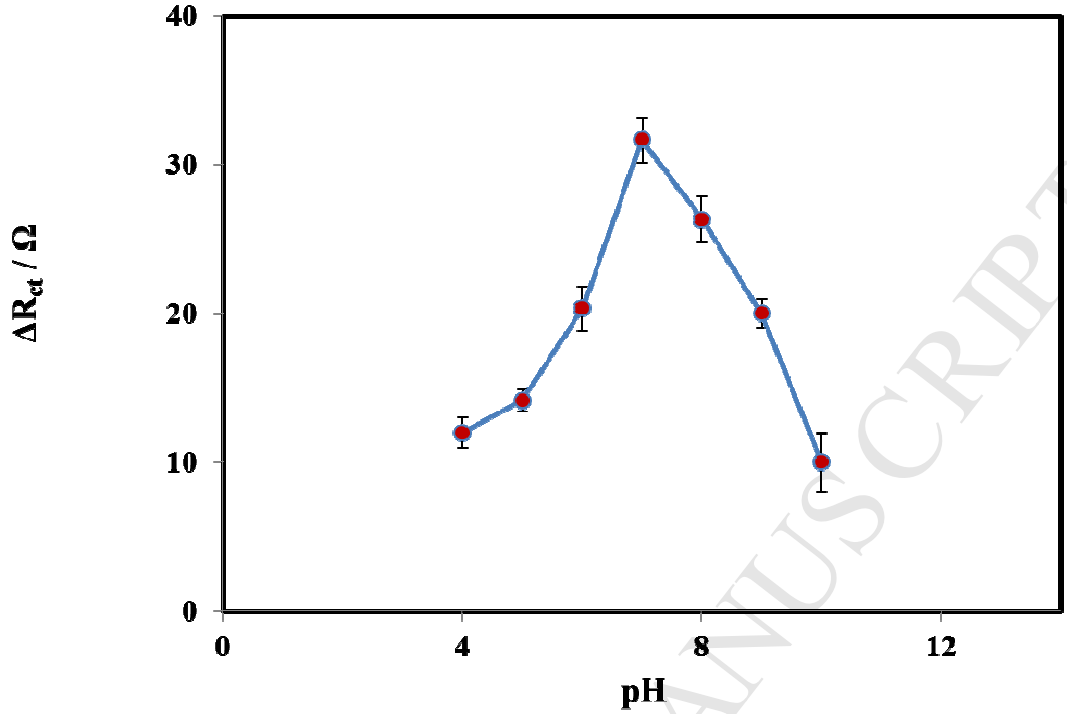

Fig. 4

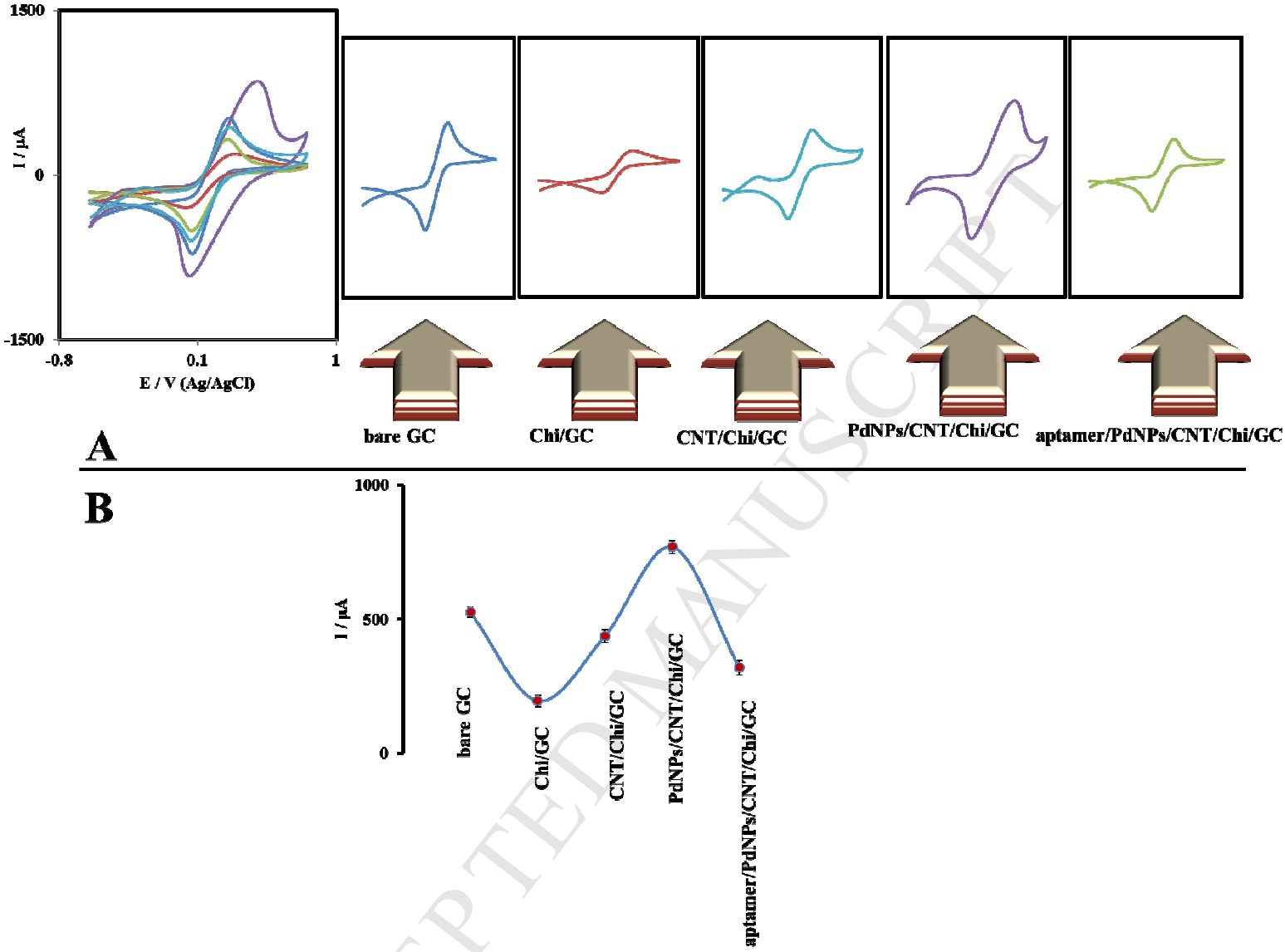

Fig. 6

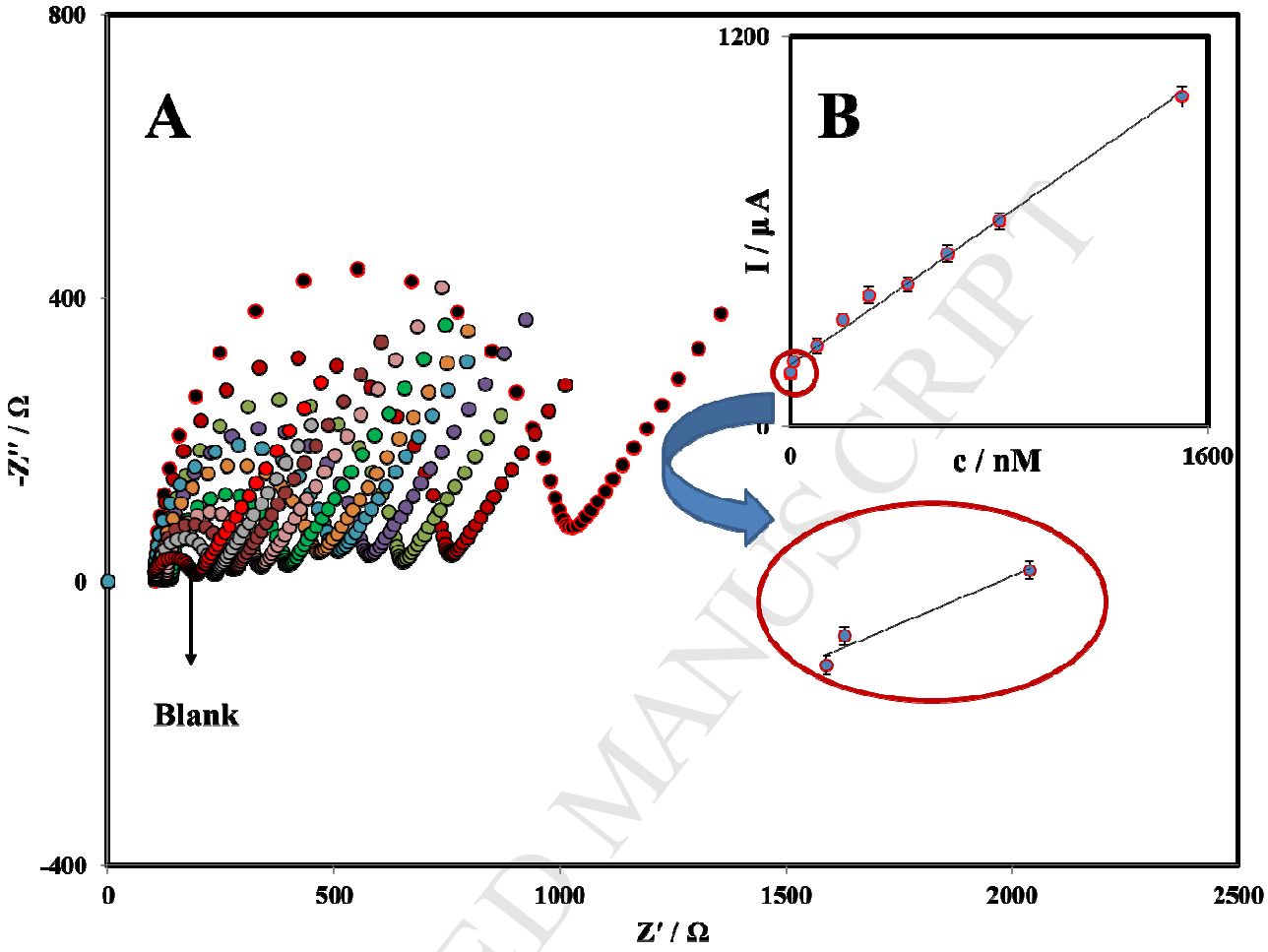

Fig. 7

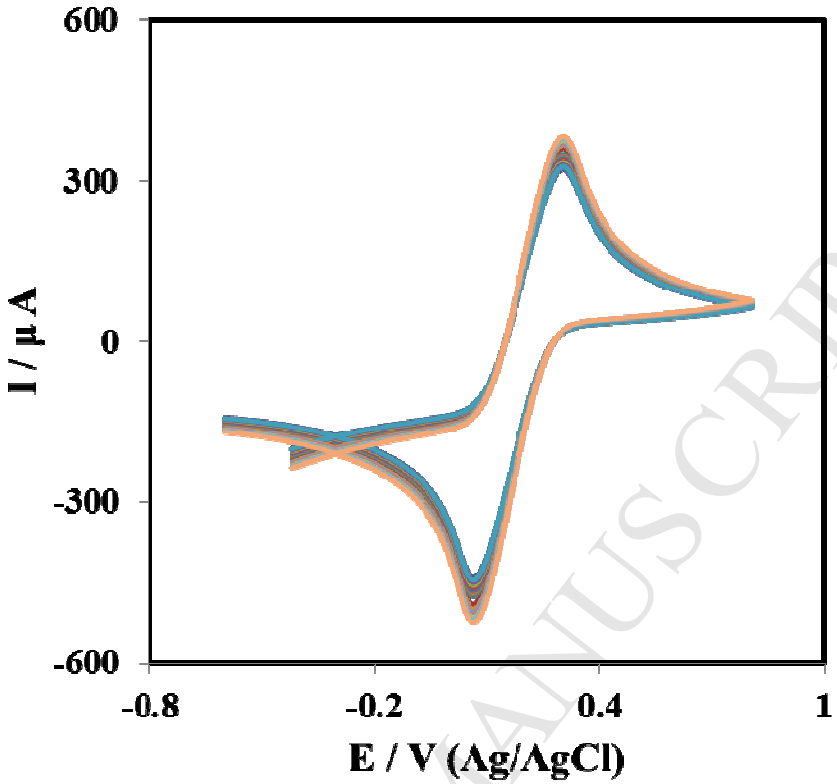

Fig. 9